Research on the Influences of the Geometric Parameters of the Vibration Isolation Effect of Miniature Concrete Vibration-Isolated Piles for Rail Transit

Jing-lei Liu, Ao-yun Wang, Chuan-qing Yu, Qian Zhao and Jian Zhang

Abstract To study the vibration isolation effect of miniature concrete vibration-isolated piles for rail transit on shallow surfaces, the evaluation parameters were set, and a model was tested to analyze different geometric parameters of vibration-isolated piles. The results show the following. When the ratio of the pile length to the wavelength is between 1.024 and 1.125, an increase in the pile length has less effect on the vibration isolation effect. When the ratio of the pile spacing to the wavelength is between 0.013 and 0.080, the vibration effect can be maintained at a good level. When the ratio of the spacing to the wavelength is greater than 0.080, the vibration isolation effect gradually decreases with an increase in the pile spacing. When the ratio of the pile section width to the wavelength is greater than 0.058, an increase in the pile section width gradually weakens the effect of the vibration isolation. Finally, when the ratio of the vibration-isolated pile section width to the pile length and the ratio between the pile spacing and the pile length are both small, vibration-isolated piles can obtain a good vibration isolation effect. Using elongated and densely arranged single-row piles can provide a good vibration isolation effect. If the location of a vibration-isolated pile is not close to the source of vibration, the pile can obtain a better vibration isolation effect. When the ratio of the vibration source distance to the pile length is in the range of 0.9–1.2, setting vibration-isolated piles at a certain distance from the vibration source can achieve a better vibration isolation effect.

J. Liu (✉) · A. Wang · C. Yu · Q. Zhao · J. Zhang
Hebei Key Laboratory of Diagnosis, Reconstruction and Anti-disaster of Civil Engineering, Zhangjiakou 075000, Hebei, China
e-mail: kingbest_1118@163.com

J. Liu · A. Wang · C. Yu · Q. Zhao · J. Zhang
School of Civil Engineering, Hebei University of Architecture, Zhangjiakou 075000, Hebei, China

E. Tutumluer et al. (eds.), *Advances in Environmental Vibration and Transportation Geodynamics*, Lecture Notes in Civil Engineering 66,
https://doi.org/10.1007/978-981-15-2349-6_2

Keywords Rail transit · Miniature concrete vibration-isolated pile · Model test · Geometric parameters

1 Introduction

1.1 A Subsection Sample

As society has progressed, rail transit has greatly developed as a more rapid mode of transportation. However, when a train passes through a building or a factory, the continuous vibration adversely affects the health of humans, the building stability, and the normal use and maintenance of precision instruments [1–4]. Many scholars have conducted various degrees of research on the effect and mechanism of the isolation of various isolation measures. Kumar et al. [5] found that the propagation mode of vibration waves in soil is based on two forms of waves, i.e., physical waves and surface waves, at the same time and that 70% of the energy is carried by surface waves. In an investigation presented by Murillo et al. [6], surface waves were the primary cause of vibration in railway operation; blocking the propagation path of surface waves in the soil can effectively reduce the impact of vibration on the surrounding environment. Wang et al. [7–10] used model tests and field tests to study the vibration characteristics of the crushed rock embankment during train operation. Hou et al. [11] used ANSYS to establish a model of an empty trench and analyzed the isolated vibration effect of empty trenches. The study found that the depth of the trenches had the greatest impact on the vibration isolation effect and that a high-frequency vibration has a better vibration isolation effect for open trenches. Zhang et al. [12] proposed a numerical method that can determine the vibration law of the soil behind open trenches in high-speed railways. The analysis of the open trench depth has a significant effect on the vibration isolation effect. Woods et al. [13] proposed using open trenches as barriers to isolate vibrations. The wavelength was studied as a parameter, and the relationship between the trench depth and the wavelength of the vibration wave on the mechanism was analyzed. Liu et al. [14, 15] used an indirect boundary integration equation method to simulate vibration isolation from several rows of elastic piles; the study found that the multiple rows of piles should be adopted for low-frequency waves, but more than three rows of piles will not significantly improve the vibration isolation effect for high-frequency waves.

However, in the above study on the isolation of vibrations, the vibration isolation effect of open trenches or row piles was regarded as a single-factor analysis. Most studies focus on a comparison of the vibration isolation effects and an analysis of the influencing factors and lack multivariate analysis of the isolation mechanisms for the vibration isolation effects.

A single-row vibration-isolated pile is used as a vibration isolation barrier in this test. The pile section size, pile length, pile spacing, and other factors are taken into account, and the test result adopts the reduction ratio of the amplitude (Ar) [13] to indicate the vibration isolation effect of the miniature concrete vibration-isolated piles.

2 Field Site and Instrumentation of the Test Layout

2.1 Field Site

Considering that the nature of sand is relatively stable in this test and the test variables are easy to control, the planar dimensions of the sand foundation form a rectangle with a size of 3 m × 2 m × 1.5 m. The planar particle size of sand is less than 5.0 mm, and the moisture content of the sand is controlled from 9 to 10%. With sand layer backfilling and then consolidation, the density of the sand is controlled from 9 to 10%.

2.2 Equipment Instrumentation

The main equipment is composed of a set of control systems named WS-Z30, which consists of a data acquisition controller, a power amplifier, an electric charge amplifier, a signal generator, an accelerometer amplifier, a signal amplifier, an electromagnetic exciter, a computer, and a few accelerometers (the sensitivity is 4 pc/ms^{-2}, the frequency response is 0.2 ~ 8000 Hz, the measurement range is 50 m/s^2, and the quality is 28.5 g). The field site and the equipment used in the experiment are shown in Figs. 1 and 2.

The pile is poured using a strength grade of C30; in this test, the pile section is designed as a square with section widths of 5, 10, and 15 cm corresponding to the

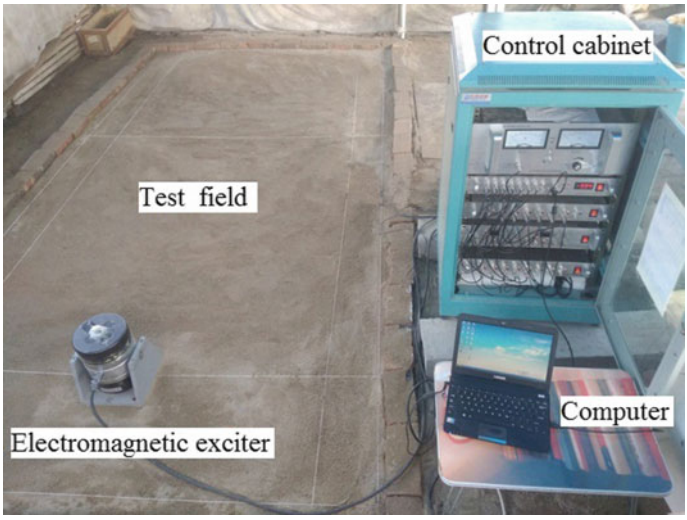

Fig. 1 Miniature concrete vibration-isolated pile and accelerometer arrangement

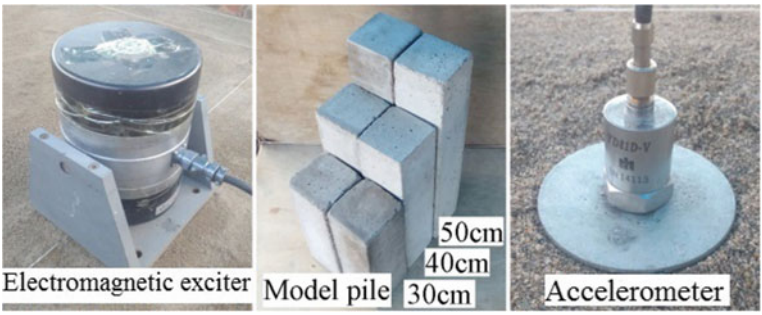

Fig. 2 Details of the test equipment

length of each section size of 30, 40, and 50 cm, respectively. There are a total of four accelerometers, and the details of the test site are shown in Fig. 3.

The excitation frequency of the exciter ranges from 10 to 150 Hz, the sampling frequency was set to 5000 times per second in the test, and the sampling time was 5 s. The charge amplifier values must be consistent in the test. The wave velocity of the excitation wave in the sand was tested in advance, and then the effect of the wavelength on the vibration isolation effect of single-row pile was analyzed.

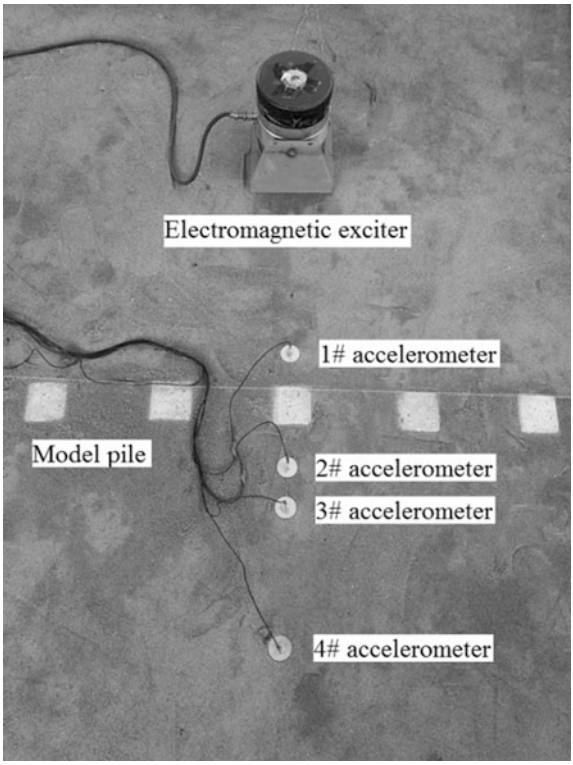

Fig. 3 Vibration-isolated pile and acceleration sensor arrangement

3 Determination of the Wave Velocity of a Soil Layer

3.1 Test Planning

This paper proposes a test method (spectral analysis of surface waves, SASW) [16, 17] to determine the wave velocity. The equipment layout that is involved is shown in Fig. 4.

Under the effect of the pulse load of the exciter, signal 1 and signal 2 were collected by the #1 accelerometer and the #2 accelerometer, respectively, and then a spectrum diagraph was obtained. Then, SASW is used to obtain the coherence function and the reciprocal power spectra of the two signals; if the coherence function value at a certain frequency exceeds the threshold value of 0.85 [16], these two signals have a significant correlation. Then, the reciprocal power spectra are used to determine the corresponding phase difference φ. Finally, the wave velocity definition is shown in Eq. (1).

$$V_R = 360 \cdot f \cdot x/\varphi \tag{1}$$

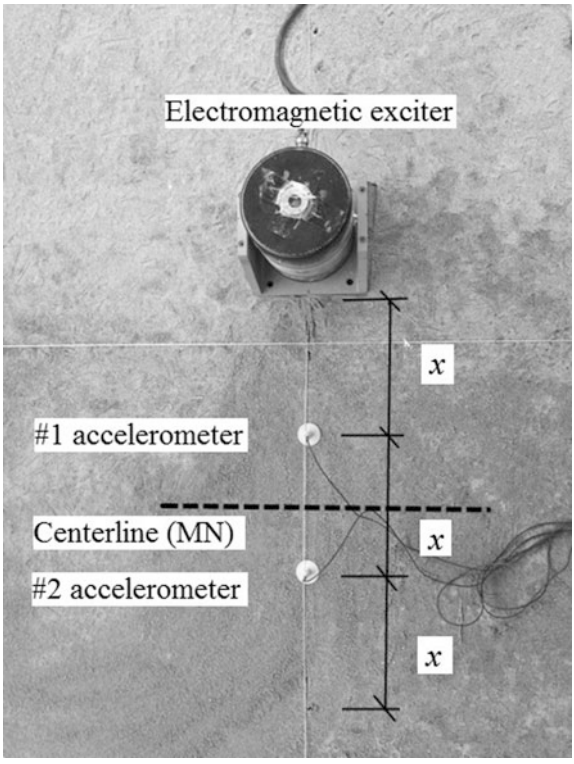

Fig. 4 Layout diagram of the test equipment

where V_R denotes the wave velocity, f denotes the excitation frequency, x denotes the distance between the #1 accelerometer and the #2 accelerometer, and φ denotes the phase difference.

The corresponding wavelength is defined as Eq. (2).

$$L_R = 360 \cdot x/\varphi \tag{2}$$

In the test, the consideration of the frequency of the source and the pile spacing mostly depends on the depth of the soil being tested [17]. Therefore, when measuring the shallow wave velocity (V_R), the vibration source is dominated by high frequencies, and the test signal is excited 4 times. The spacing (x) is in turn taken from Table 1. The forward test direction is defined as being from the #1 accelerometer to the #2 accelerometer. After the forward test is finished, the position of the accelerometer is not changed, the exciter is moved symmetrically to the other side of the centerline (MN), and then the above operation is repeated in the backward. The testing conditions are shown in Table 1.

3.2 Data Processing

Taking testing condition 5 from Table 1 as an example, the exciter is arranged on the right side of the centerline (MN). The coherence function to analyze the measured signals, i.e., signal 1 and signal 2, and the coherent coefficient corresponding to the excitation frequency of 150 Hz from the derived frequency-domain files are screened. The coherence function is shown in Fig. 5.

The value of 0.956 marked in Fig. 5 represents the coherence coefficient value of the corresponding signal when the excitation wave propagates from the #1 accelerometer to the #2 accelerometer under testing condition 5. The requirement that the coherence coefficient value is greater than 0.85 is satisfied [16]; then, the phase difference φ was found using the method of the cross-power spectrum. The cross-power spectrum is shown in Fig. 6.

Table 1 Testing conditions of the wave velocity test

Testing conditions	Frequency f (Hz)	Spacing x (cm)	Test direction
1	140	30	Forward
2	140	30	Forward
3	140	40	Forward
4	140	40	Forward
5	150	30	Backward
6	150	30	Backward
7	150	40	Backward
8	150	40	Backward

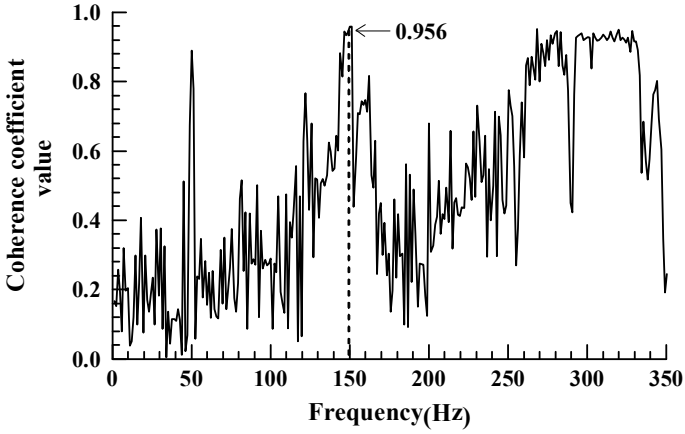

Fig. 5 Coherent function of testing condition 5

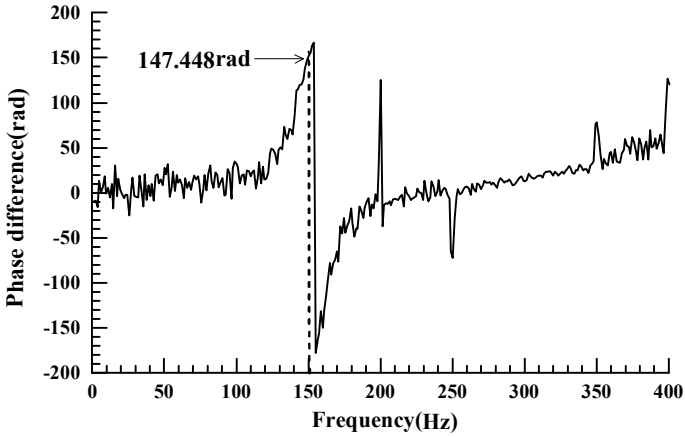

Fig. 6 Reciprocal power spectrum of testing condition 5

The value of 146.457 rad marked in Fig. 6 represents the phase difference (φ) value of the corresponding signal when the excitation wave propagates from the #1 accelerometer to the #2 accelerometer under testing condition 5.

Using the same method for the remaining conditions in Table 1, the arithmetic mean of the test results is taken in both directions as the measured wave velocities on the surface of the soil. The wave velocities are shown in Table 2.

After averaging the wave velocities (V_R) that were measured at each operating condition, the arithmetic mean was 109.989 m/s.

Table 2 Results of the wave velocity test

Testing conditions	Coherence value	Phase difference φ (rad)	Wave velocity V_R (m/s)	Arithmetic mean (m/s)
1	0.956	147.448	109.870	109.989
2	0.988	146.669	110.453	
3	0.976	147.748	109.646	
4	0.964	145.993	110.964	
5	0.975	247.443	109.116	
6	0.972	245.716	109.883	
7	0.968	248.187	108.789	
8	0.976	242.83	110.189	

4 Size Optimization of a Single Factor

4.1 Single-Factor Data Processing

The reduction ratio of the amplitude (Ar) is adopted to indicate the vibration isolation effect of a single-row vibration-isolated pile. A smaller Ar indicates that the vibration isolation effect of single-row piles is better [13].

The Ar is defined as in Eq. (3).

$$Ar = a_1/a_o \tag{3}$$

where a_1 denotes the vertical vibration acceleration of the ground after setting a single-row vibration-isolated pile and a_o denotes the vertical vibration acceleration of the free field that is excited in the same position.

The influences on the vibration isolation effect of the length of the pile (L), the size of the pile section ($B \times B$), the pile spacing (s), the distance from the vibration source (r), and the wavelength (L_R) are investigated. The following parameters are introduced to evaluate the effects of vibration isolation and are used as a measure of the vibration isolation effect of the vibration-isolated piles.

(1) **Depth parameter *D***

The ratio D between the length (L) of the pile and the wavelength (L_R) represents the effect of different lengths of the piles on the vibration isolation effect of the vibration-isolated piles. The formula is shown in Eq. (4).

$$D = L/L_R \tag{4}$$

(2) **Width parameter *W***

The ratio W between the width (B) of the pile and the wavelength (L_R) represents the influence of the different widths of the piles on the vibration isolation effect of the vibration-isolated piles. The formula is shown in Eq. (5).

$$W = B/L_R \tag{5}$$

(3) **Pile spacing parameter *S***

The ratio S between the pile spacing (s) and the wavelength (L_R) indicates the influence of the density of the pile arrangement on the isolation effect of the vibration-isolated piles. The formula is shown in Eq. (6).

$$S = s/L_R \tag{6}$$

(4) **Vibration source distance parameter *K***

The ratio K between the distance from the vibration source (r) and the wavelength (L_R) indicates the influence of the distance from the vibration-isolated pile to the vibration source on the vibration-isolated effect of the piles. The formula is shown in Eq. (7).

$$K = r/L_R \tag{7}$$

4.2 Influence of the Depth Parameter on the Vibration Isolation Effect of Piles

The length of the pile is the main factor that influences the vibration isolation effect [18]. First, the distance from the vibration source (r), the width of the pile section (B), and the pile spacing (s) were controlled. The effects of the pile length (L) on the vibration isolation of the pile were studied separately; the test arrangement is shown in Table 3.

The excitation frequency of the exciter ranges from 10 to 150 Hz; 10 Hz is used as the step length for gradual excitations. After the discrete data are removed, the remaining data are fitted using MATLAB. Under certain conditions, the regression

Table 3 Test arrangement of the parameter D

Testing conditions	Distance from the vibration source r (cm)	Section width of piles φ (cm)	Pile spacing s (cm)
1	60	15	10
2	50	10	10
3	35	5	10

Table 4 Correlation analysis for D and Ar

Category	Testing condition 1	Testing condition 2	Testing condition 3
Regression equation	$Ar = 0.069D^{-1.334}$	$Ar = 0.068D^{-1.413}$	$Ar = 0.065D^{-1.406}$
Degree of freedom (f)	40	42	39
Significance level (α)	0.05	0.05	0.05
Correlation coefficient (R)	0.9672	0.9465	0.9266
Critical value ($R_{\alpha,f}$)	0.3044	0.2973	0.3081
F	4.9531	4.3524	4.5426
F_α	4.0800	4.0720	4.0980

equations of the depth parameter (D) and the Ar are shown in Table 4. Significance tests on the regression equation were calculated to verify the correlations between the variables. The correlation coefficient R and the F value were derived using MATLAB. The correlation coefficient R and the F value are used to judge the statistical significance of the regression equation; if the correlation coefficient R is greater than the critical value $R_{\alpha,f}$ and closer to 1 and if the F value is greater than the critical value F_α, the regression equation is more obvious and the fitting is better. The $R_{\alpha,f}$ and F_α values of each testing condition are identified by using the tables of correlation coefficient critical values [19] and the F distribution table [19], as shown in Table 4.

Under testing conditions 1, 2, and 3, the correlation coefficient R is greater than the critical value of $R_{\alpha,f}$, and the value of F is greater than the value of F_α from Table 4. The results show that the regression equation is significant in each testing condition; thus, the regression equation is meaningful and can be accepted.

The fitting graph of the regression equation for various testing conditions is shown in Fig. 7.

Figure 7 shows D rapidly increasing from approximately 0.18 to 0.8 and the value of Ar decreasing rapidly. When D increasing to approximately 0.8, the change in Ar tends to flatten gradually, and when D is in the approximate range of 1.042–1.125, the slope of the fitting curve is approximately $Ar' \approx 0$. When the length of the pile (L) increases, the change in Ar tends to be stable. When the length of the pile (L) continues to increase, the influence of the vibration isolation effect will be weakened. Under the conditions of controlling other influencing factors, $D = 1.042$ can be used as the limiting range of the length of the effective pile body.

4.3 Influence of the Pile Spacing Parameter on the Vibration Isolation Effect of Piles

The distance between the nearest edges of adjacent piles obviously influences the vibration isolation effect of the vibration-isolated pile. According to the

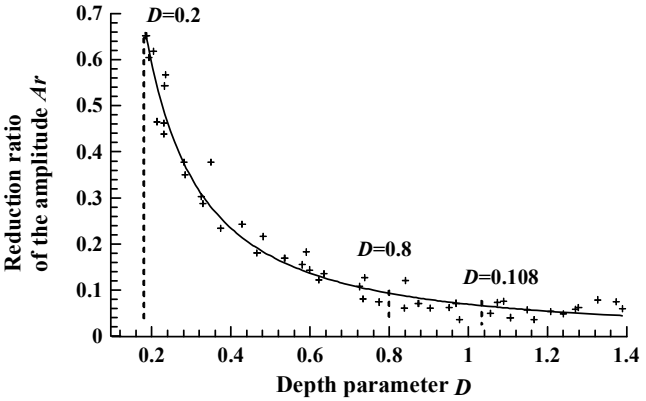

(a) Fitting curve of D and Ar under testing condition 1

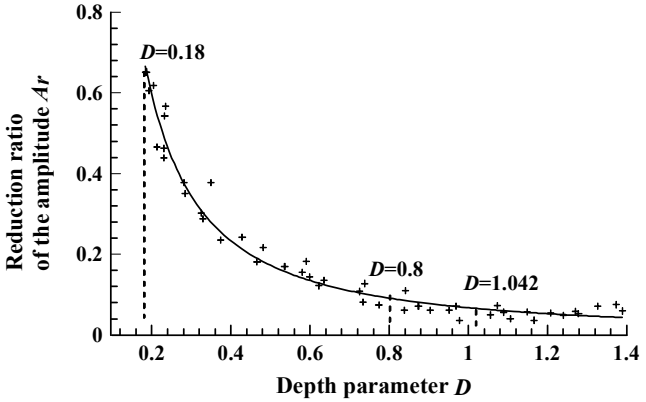

(b) Fitting curve of D and Ar under working condition 2

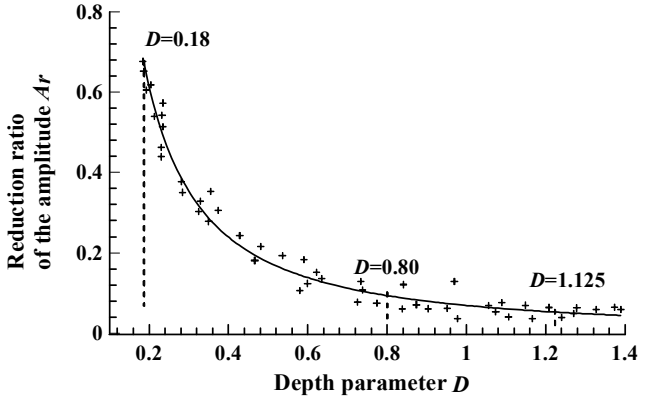

(c) Fitting curve of D and Ar under testing condition 3.

Fig. 7 Fitting curve of D and Ar

Table 5 Test arrangement of the parameter S

Testing conditions	Distance from the vibration source r (cm)	Section width of piles B (cm)	Pile of the length L (cm)
1	60	15	50
2	50	10	50
3	35	5	50

Table 6 Correlation analysis of S and Ar

Category	Testing condition 1	Testing condition 2	Testing condition 3
Regression equation	$Ar = 0.119 - 1.071S + 9.029S^2$	$Ar = 0.118 - 1.257S + 8.906S^2$	$Ar = 0.093 - 0.936S + 9.015S^2$
Degree of freedom (f)	38	41	40
Significance level (α)	0.05	0.05	0.05
Correlation coefficient (R)	0.9412	0.9532	0.9715
Critical value ($R_{\alpha,f}$)	0.3120	0.3008	0.3044
F	4.5143	4.6462	4.6523
F_α	4.098	4.076	4.080

optimization method of controlling other variables, the pile spacing parameter S is processed. The specific testing conditions are shown in Table 5.

The excitation method of the parameter S is the same as the parameter D in the test arrangement. Additionally, the discrete data are removed, and then the remaining data are fitted. Under certain conditions, the regression equations of the parameter S and the Ar are shown in Table 6. Statistical significance of the test is shown in Table 6.

Table 6 shows that the correlation coefficient R is greater than the critical value of $R_{\alpha,f}$ and that the F values are greater than the value of F_α. These results show that the regression equation is significant in each testing condition; thus, the regression equation is meaningful and can be accepted.

The fitting graphs of the regression equations for the various testing conditions are shown in Fig. 8.

Figure 8 shows that when S is increasing from approximately 0.013 to 0.0804, the value of Ar changes slowly and sustains a lower level, demonstrating that a single-row pile can obtain a better vibration isolation effect. After S increases to approximately 0.0804, the change in Ar tends to grow rapidly, and then the vibration isolation effect decreases gradually. Under the conditions of controlling other influencing factors, the pile spacing (s) can be maintained at a lower level ($S = 0.013$), while the better vibration isolation effect can be obtained.

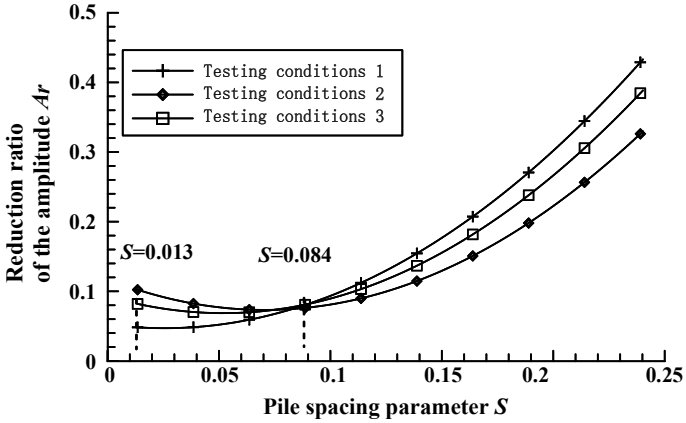

Fig. 8 Fitting curve of S and Ar

4.4 *Influence of the Width Parameter on the Vibration Isolation Effect of Piles*

The influence of the width parameter (W) on the vibration isolation of vibration-isolated piles is studied; the test arrangement is shown in Table 7.

The excitation method of the parameter W is the same as the parameter D in the test arrangement. Additionally, the discrete data are removed, and then the remaining data are fitted. Under certain conditions, the regression equations of the parameter W and the Ar are shown in Table 8. The statistical significance of the test is shown in Table 8.

Table 8 shows that the correlation coefficient R is greater than the critical value of $R_{\alpha,f}$ and that the F values are greater than the value of F_{α}. The results show that the regression equation is significant in each testing condition; thus, the regression equation is meaningful and can be accepted.

The fitting graphs of the regression equations for the various testing conditions are shown in Fig. 9.

Figure 9 shows that when W is increasing from approximately 0.004 to 0.058, the value of Ar increases rapidly. Additionally, the vibration isolation effect is weakened rapidly. W increases to approximately 0.058, and with an increase in W, the change in

Table 7 Test arrangement of the parameter W

Testing conditions	Distance from the vibration source r (cm)	Pile length L (cm)	Pile spacing s (cm)
1	60	50	10
2	50	40	10
3	35	30	10

Table 8 Correlation analysis of W and Ar

Category	Testing condition 1	Testing condition 2	Testing condition 3
Regression equation	$Ar = 0.689\ W^{0.106}$	$Ar = 0.694\ W^{0.1562}$	$Ar = 0.632\ W^{0.166}$
Degree of freedom (f)	37	40	41
Significance level (α)	0.05	0.05	0.05
Correlation coefficient (R)	0.9345	0.9563	0.9641
Critical value ($R_{\alpha,f}$)	0.3160	0.3044	0.3008
F	4.2351	4.5474	4.3542
F_α	4.107	4.08	4.076

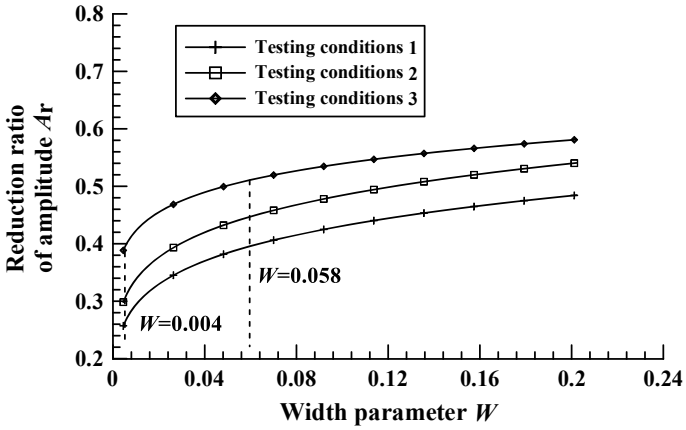

Fig. 9 Fitting curve of W and Ar

Ar tends to gradually shallow. In other words, with an increase in the width of a square pile, the change in the vibration isolation effect is not significant. This is similar to the conclusion of Hou En-ping's [18] study that a single-row vibration-isolated pile section size change has no significant influence on the vibration isolation effect. When the vibration-isolated pile is practically engineered, choosing a reasonable section size of vibration-isolated pile is of guiding significance.

4.5 Influence of the Vibration Source Distance Parameter on the Vibration Isolation Effect of Piles

When a vibration wave is transmitted over a distance and the energy of the wave is consumed continuously, it is advantageous to improve the vibration isolation effect

Table 9 Test arrangement of the parameter K

Testing conditions	Section width of piles B (cm)	Pile length L (cm)	Pile spacing s (cm)
1	15	50	10
2	10	40	10
3	5	30	10

Table 10 Correlation analysis of K and Ar

Category	Testing condition 1	Testing condition 2	Testing condition 3
Regression equation	$Ar = 0.409 - 0.742K + 1.221K^2$	$Ar = 0.375 - 0.992K + 1.463K^2$	$Ar = 0.449 - 0.720K + 1.213K^2$
Degree of freedom (f)	40	41	39
Significance level (α)	0.05	0.05	0.05
Correlation coefficient (R)	0.9561	0.9436	0.9674
Critical value ($R_{\alpha,f}$)	0.3044	0.3008	0.3081
F	4.1124	4.3513	4.8521
F_α	4.08	4.076	4.08

by arranging the positions of the vibration-isolated piles rationally. The specific testing conditions are shown in Table 9.

The excitation method of the parameter K is the same as the parameter D in the test arrangement. Additionally, the discrete data are removed, and then the remaining data are fitted. Under certain conditions, the regression equations of K and Ar are shown in Table 10. The statistical significance of the test is shown in Table 10.

Table 10 shows that the correlation coefficient R is greater than the critical value of $R_{\alpha,f}$ and that the F values are greater than the value of F_α. The results show that the regression equation is significant in each testing condition; thus, the regression equation is meaningful and can be accepted. The fitting graphs of the regression equations for the various testing conditions are shown in Fig. 10.

Figure 10 shows that when K rapidly increases from approximately 0.031 to 0.291, the value of Ar shows a decreasing phenomenon, and when K increases in the approximate range from 0.291 to 0.357, regions of minima occur, and the vibration isolation effect is relatively excellent. When K increases to approximately 0.357, the change in Ar tends to increase gradually. Under the conditions of controlling other influencing factors, K values between 0.291 and 0.357 can be used as a reference index for determining the reasonable positions of vibration-isolated pile.

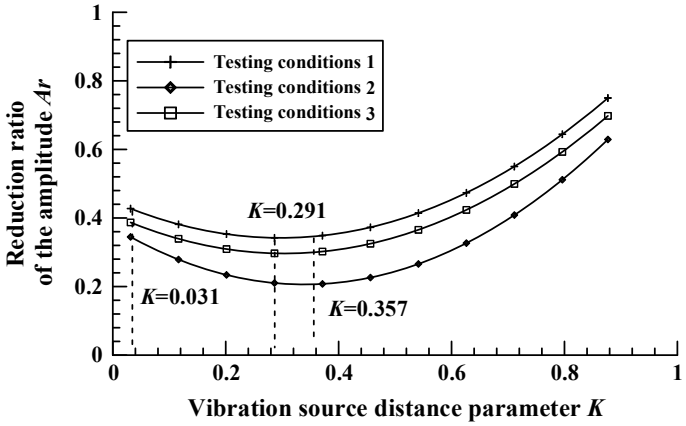

Fig. 10 Fitting curve of K and Ar

5 Size Optimization of Two Factors

5.1 Two-Factor Data Processing

In single-factor analysis, the influences of the pile length (L), the pile cross-sectional size ($B \times B$), the pile spacing (s), and the vibration source distance (r) on the vibration isolation effect of the single-row pile are analyzed individually. The influence of the pile length (L) on the vibration isolation effect is the most obvious.

Therefore, the parameters of the two-factor analysis are introduced into the length of the pile using the single-factor analysis results of the reasonable pile length (L) range and are then used to define the reasonable range of the section width (B), the pile spacing (s), and the vibration source distance (r).

The setting parameters are as follows:

(1) **Slenderness ratio δ**

The ratio δ between the section width (B) and the length of the pile (L) represents the degree of elongation of the pile. The formula is shown in Eq. (8).

$$\delta = B/L \tag{8}$$

(2) **Relative spacing of piles β**

The ratio β between the pile spacing (s) and the length of the pile (L) represents the single-row piles' layout density. The formula is shown in Eq. (9).

$$\beta = s/L \tag{9}$$

(3) **Relative vibration source distance γ**

The ratio γ between the distance from the vibration source (r) and the length of the pile (L) represents the position of a single-row pile relative to the vibration source. The formula is shown in Eq. (10).

$$\gamma = r/L \tag{10}$$

5.2 *Influence of the Slenderness Ratio δ on the Vibration Isolation Effect of the Piles*

The vibration isolation effect of the pile width and the length of the pile were studied by preparing a test group and a control group, respectively. The test results of the experimental group were validated by the test results of the control groups. The specific testing conditions are shown in Table 11.

In the test and control groups, the section width of the pile was 5, 10, or 15 cm corresponding to a length of each section size of 30, 40, and 50 cm, respectively; the ratio δ has nine kinds of values. Vibration frequencies of 10, 50, and 100 Hz were selected, and then the vibration frequencies were tested. The vibration isolation effect of each testing condition was compared. The results of the test are shown in Figs. 11 and 12.

Figure 11 shows that the corresponding graphs of the two groups show a similar trend. When δ is between 0.1 and 0.2, corresponding value of Ar changes gently. When δ is greater than 0.2, the value of Ar increases rapidly with the δ. For each high, medium, and low frequency, the rule is consistent insomuch that the value of Ar increases with δ, showing a smooth change in a certain interval and then an increasing phenomenon.

Figure 12 shows that the change laws of the corresponding figures in the test and control groups are consistent with those of the two groups.

Using both Figs. 11 and 12 and further analyzing the test results, it is found that when the size of the pile has a smaller δ for a vibration-isolated piles, it can obtain a

Table 11 Test arrangement of the parameter δ

Testing conditions	Test group		Testing conditions	Control group	
	Pile spacing s (cm)	Distance from the vibration source r (cm)		Pile spacing s (cm)	Distance from the vibration source r (cm)
1	10	50	3	15	50
2	10	60	4	15	60

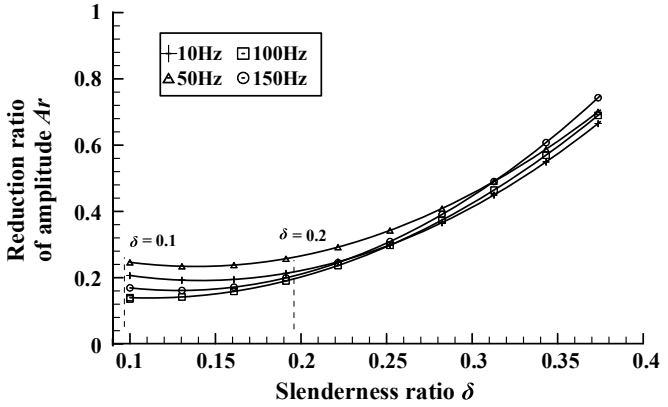

(a) Changing relation between Ar and δ for testing condition 1

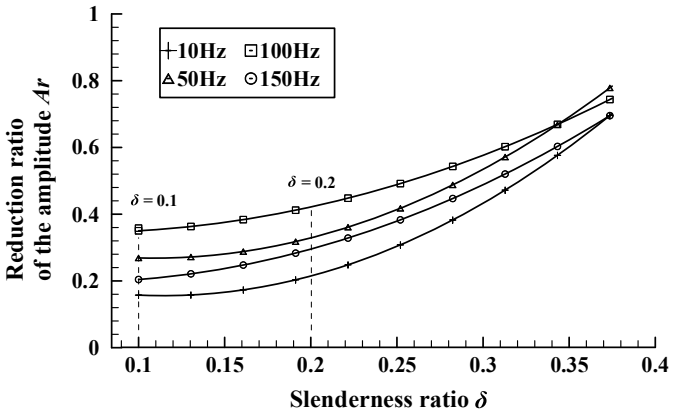

(b) Changing relation between Ar and δ for testing condition 2

Fig. 11 Changing relation between Ar and δ in the experimental group

better vibration isolation effect; when the size of the vibration-isolated pile is less than δ, the vibration isolation effect of a vibration-isolated pile is weakened. The vibration isolation effect of the vibration-isolated pile is maintained at a good level when δ is kept between 0.1 and 0.2.

5.3 Influence of the Relative Spacing of the Piles β on the Vibration Isolation Effect of the Piles

The relative spacing of the pile (β) reflects the influence of the density of the vibration-isolated piles on the vibration isolation effect. To study the relationship

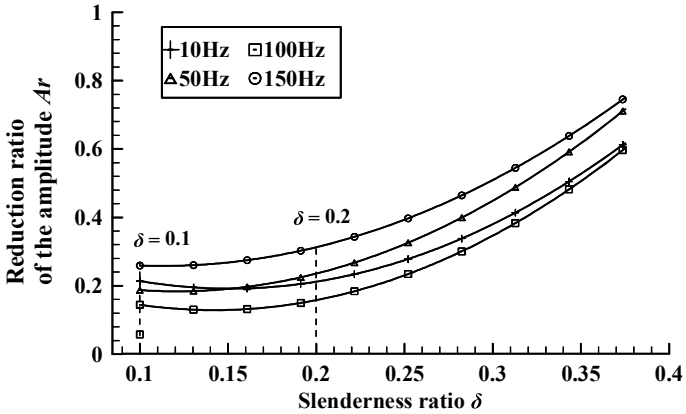

(a) Changing relation between Ar and δ for testing condition 3

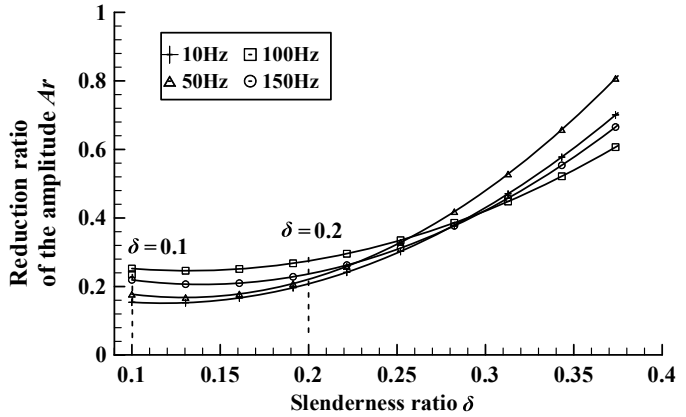

(b) Changing relation between Ar and δ for testing condition 4

Fig. 12 Changing relation between Ar and δ in the control group

between β and Ar, the test group and control group were prepared; the test arrangement is shown in Table 12.

The specifications of the vibration-isolated pile and the excitation frequencies used in the test are the same as the arrangement of the δ test, and the test results are shown in Figs. 13 and 14.

Figure 13 shows that the corresponding figures of the two group testing conditions show a similar trend in the two group testing conditions for the test group. For each of the high, medium, and low excitation frequencies in the figure, the value of Ar increases rapidly with an increase in β.

Figure 14 shows that the change laws of the corresponding figures in the test and control groups are consistent with those of the two groups.

Table 12 Test arrangement of the parameter β

Testing conditions	Test group		Testing conditions	Control group	
	Section width B (cm)	Distance from the vibration source r (cm)		Section width B (cm)	Distance from the vibration source r (cm)
1	10	50	3	15	50
2	10	60	4	15	60

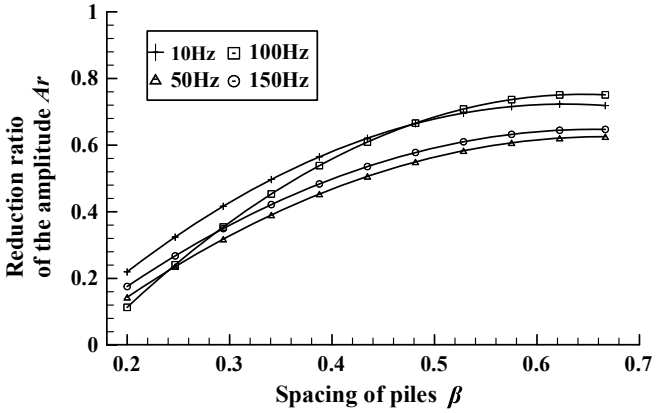

(a) Changing relation between Ar and β for testing condition 1

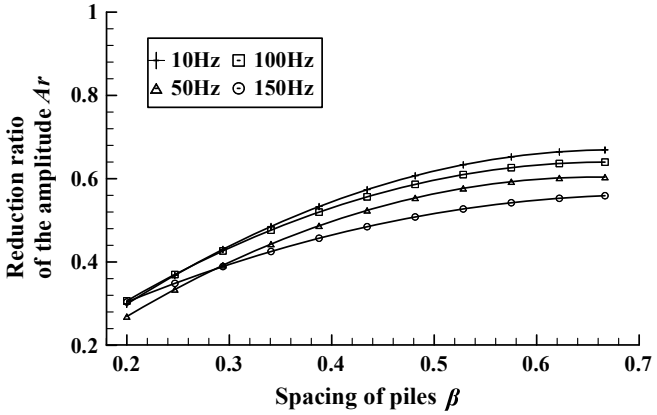

(b) Changing relation between Ar and β for testing condition 2

Fig. 13 Changing relation between Ar and β for the experimental group

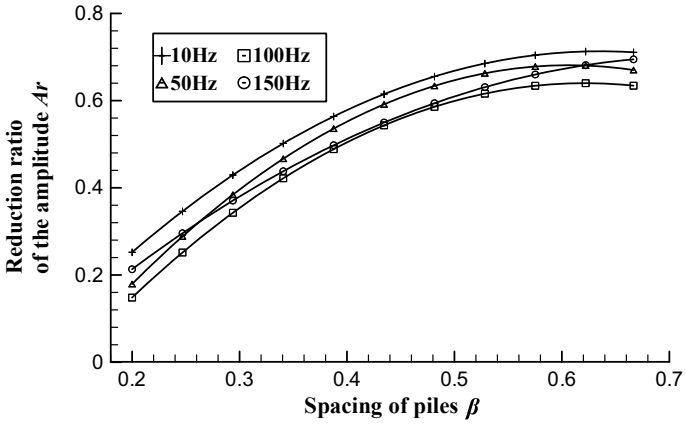

(a) Changing relation between Ar and β for testing condition 3

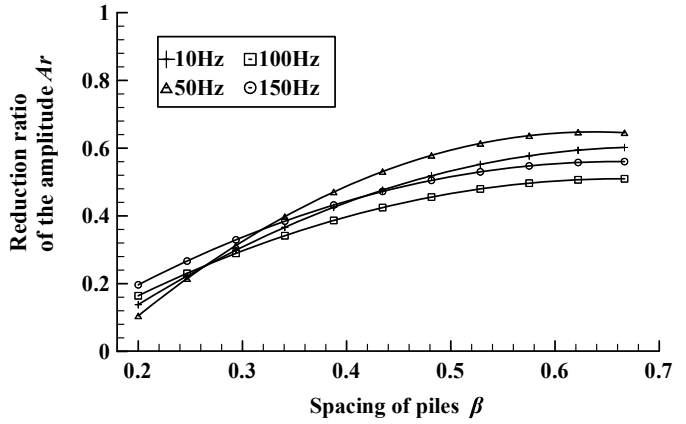

(b) Changing relation between Ar and β for testing condition 4

Fig. 14 Changing relation between Ar and β for the control group

Using both Figs. 13 and 14, it is found that when β is small, the single-row pile has a better isolation effect when adopting a long pile and a dense arrangement; when β is large, the isolation effect of the vibration-isolated pile will weaken when a sparse arrangement of short piles is used.

Table 13 Test arrangement of the parameter γ

Testing conditions	Test group		Testing conditions	Control group	
	Section width B (cm)	Pile spacing s (cm)		Section width B (cm)	Pile spacing s (cm)
1	10	10	3	15	10
2	10	15	4	15	15

5.4 *Influence of the Relative Vibration Source Distance γ on the Vibration Isolation Effect of the Piles*

The relative vibration source (γ) reflects the influence of the arranged positions of vibration-isolated piles on the vibration isolation effect. The test group and control group were prepared to study the relationship between γ and Ar; the test arrangement is shown in Table 13.

The specifications of the vibration-isolated pile and the excitation frequencies used in the test are the same as those in the arrangement of the δ test; the test results are shown in Figs. 15 and 16.

Figure 15 shows that the corresponding figures of two group testing conditions show similar trends in the two group testing conditions for the test group. For each of the high, medium, and low excitation frequencies in the figure, γ rapidly grows from approximately 0.7 to 0.9, and the value of Ar decreases gradually with an increase in γ. When γ increases from approximately 0.9 to 1.2, regional minima are presented, and when γ increases to approximately 1.2, with an increase in γ, the change in Ar tends to increase gradually.

Figure 16 shows that the change laws of the corresponding figures in the test and control groups are consistent with those of the two groups.

Using both Figs. 15 and 16, it is found that if the position of the vibration-isolated pile is not closer to the vibration sources, a better vibration isolation effect can be obtained by a vibration-isolated pile. However, when the layout of the vibration-isolated pile satisfies the requirement that the γ reaches the range of 0.9–1.2, it can obtain a better vibration isolation effect.

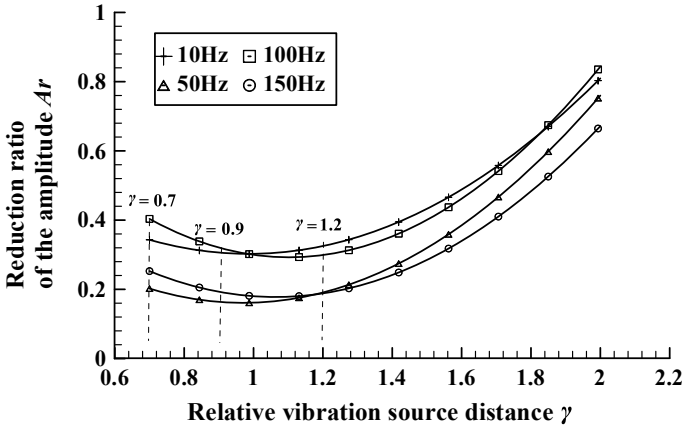

(a) Changing relation between Ar and γ for testing condition 1

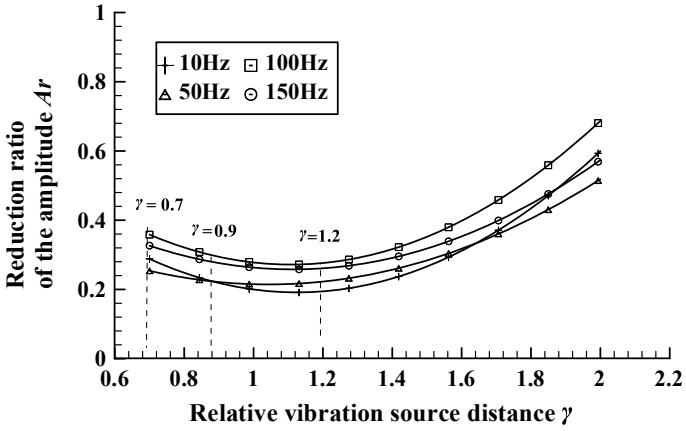

(b) Changing relation between Ar and γ for testing condition 2

Fig. 15 Changing relation between Ar and γ for the experimental group

6 Conclusions

To study each of the factors that affect the vibration isolation effect of a concrete vibration-isolated pile, single-factor analysis and two-factor analysis methods are applied on model tests while considering the length of the pile and the pile cross section; the following conclusions are obtained:

(1) When D increases to approximately 1.042–1.125, the change in Ar tends to become stable with an increase in the length of the pile (L). When the length of the pile (L) continues to increase, the enhancement of the vibration isolation

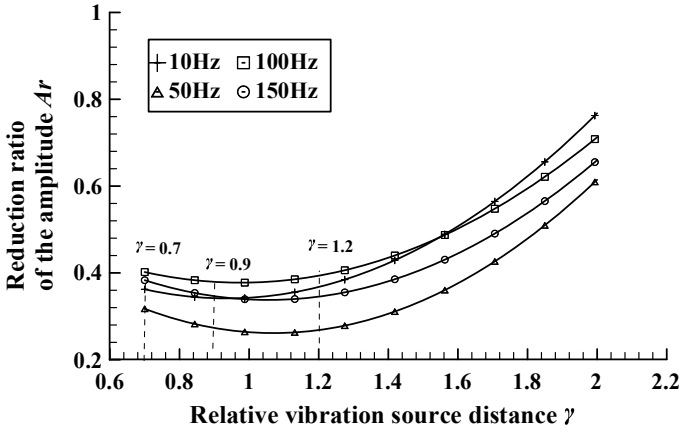

(a) Changing relation between Ar and γ for testing condition 3

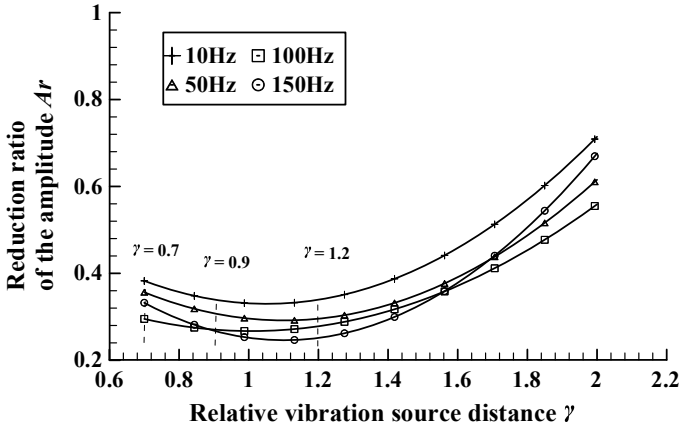

(b) Changing relation between Ar and γ for testing condition 4

Fig. 16 Changing relation between Ar and γ for the control group

effect will be nonsignificant. When the depth parameter (D = 1.042) can be used as the limit range of the length of the effective pile body, a better vibration isolation effect can be obtained.

(2) When the width of a vibration-isolated pile increases, the change in the vibration isolation effect is not significant; when the vibration-isolated pile is furnished and the pile spacing (s) is bigger, the vibration isolation effect will weaken.

(3) When the position of a vibration-isolated pile is not closer to the vibration source, a better vibration isolation effect can be obtained by a vibration-isolated pile. When K is between 0.291 and 0.357, it can be used as a reference index for determining reasonable positions of vibration-isolated piles.

(4) The vibration-isolated pile length (L) has the most obvious influence on the vibration isolation effect when increasing the length of the vibration-isolated pile, and Ar can reach levels below 0.1.
(5) When the slenderness ratio (δ) is between 0.1 and 0.2, a vibration-isolated pile can obtain a better vibration isolation effect, and the minimum value of Ar can reach 0.2. If the relative pile spacing (β) is larger, the vibration isolation effect of a vibration-isolated pile is worse.
(6) If the location of a vibration-isolated pile is not close to the source of vibration, the vibration-isolated pile can obtain a better vibration isolation effect, and if the relative vibration source distance (γ) is between 0.9 and 1.2, the value of Ar can reach $0.3 \sim 0.4$.

Acknowledgements This paper was supported by the Youth Talent Projects of Colleges in Hebei Province of China (No. BJ2016018) and the Hebei University of Architecture Graduate Innovation Fund (No. XA201913).

References

1. Ma M, Liu WN, Wang WB et al (2016) Evaluation of train-induced environmental vibrations considering the factor of exposure time. J Vib Shock 35(11):207–211
2. Hong JQ, Liu WQ, Wang SG (2008) Vibration analysis of base-isolated building near urban rail transit. J Vib Shock 27(11):37–50
3. Ma LH (2014) Research on vibration of Shanghai-Nanjing intercity high-speed railway and its environment impact. Beijing Jiaotong University, Beijing
4. Ma LH, Liang QH, Gu AJ et al (2015) Research on impact of Shanghai-Nanjing intercity high-speed railway induced vibration on ambient environment and foundation settlement of adjacent Beijing-Shanghai railway. J China Railw Soc 37(2):98–105
5. Kumar P, Sand HK, Chakraborty SK (2014) Isolation of plane shear wave using water saturated trench barrier. Soil Dyn Earthq Eng 59:42–50
6. Murillo C, Thorel L, Caicedo B (2009) Ground vibration solation with geofoam barriers centrifuge modeling. Geotext Geomembr 27(6):423–434
7. Wang QY, Zhang JS, Meng F et al (2013) Simulation of train vibration load on the subgrade testing model of high-speed railway. J Vib Shock 32(6):43–46
8. Zhan YX, Jiang GL (2010) Study of dynamic characteristics of soil subgrade bed for ballastless track. Rock Soil Mech 31(2):392–396
9. Gao GY, Li ZY, Feng SJ et al (2007) Experimental results and numerical predictions of ground vibration induced by high-speed train running on Qin-Shen railway. Rock Soil Mech 28(9):11817–11822
10. Qu CZ, Wang YH, Wei LM et al (2012) In-situ test and analysis of vibration of subgrade for Wuhan-Guangzhou high-speed railway. Rock Soil Mech 33(5):1451–1456
11. Hou DJ, Lei XY, Luo XW (2006) The numerical analysis of railway vibration by trenches. J Railw Sci Eng 3(2):48–52
12. Zhang LG, Liu JL, Song XG et al (2017) The numerical analysis of effect and influencing factor of vibration by open trench on high-speed railway. J Railw Sci Eng 14(7):1356–1359
13. Woods RD, Barnett NE, Sangesser R (1974) Holography, a new tool for soil dynamics. J Geotech Eng Div ASCE 100(11):1234–1247

14. Liu ZX, Wang SJ (2016) Isolation effect of discontinuous pile-group barriers on plane P and SV waves: simulation based on 2D broadband indirect boundary integration equation method. Rock Soil Mech 37(4):1195–1207
15. Li ZY, Gao GY, Qiu C et al (2006) Analysis of multi-row of piles as barriers for isolating vibration in far field. Chin J Rock Mech Eng 24(21):3990–3995
16. Wu SM, Zeng GX, Chen YM et al (1988) Measurement of wave velocity of soil deposits by spectral analysis of surface waves. Earthq Eng Eng Vib 8(4):28–31
17. Chen YM, Wu SM, Zeng GX (1992) Spectral analysis of surface waves and its application. China J Geotech Eng 14(3):61–64
18. Hou EP, Liu JL, Zhang RH et al (2017) Model test study on vibration isolation effect of concrete rows piles for railway subgrade. Railw Eng (3):141–145
19. He W, Xue WD, Tang B (2015) Optimization test design method and data analysis, 1st edn. Chemical Industry Press, Beijing